A PARYLENE CUFF ELECTRODE FOR PERIPHERAL NERVE RECORDING AND DRUG DELIVERY

Angelica M. Cobo[1], Barbara Boyajian[1], Christopher Larson[1], Kee Scholten[1], Victor Pikov[2], and Ellis Meng[1]*

[1]University of Southern California, Los Angeles, California, USA

[2]Galvani Bioelectronics, UK

ABSTRACT

We present a novel polymer-based cuff electrode designed for peripheral nerve recording and drug delivery. The micromachined cuff interface consists of platinum electrodes embedded within Parylene microfluidics. An adjustable locking mechanism ensures close-fitting of the cuff around the nerve for localized drug delivery to induce axonal sprouting from the fascicles towards the embedded electrodes. This Lyse-and-Attract Cuff Electrode (LACE) specifically incorporates drug delivery to improve sensitivity, spatial resolution, fascicle selectivity, and chronic reliability over existing electrode-only interfaces. We present the design, fabrication, and initial testing of fully functional cuffs including evaluation of the locking mechanism, localized drug delivery, and electrochemical properties of recording electrodes.

INTRODUCTION

Prostheses for amputees based on implantable peripheral nerve (PN) interfaces have the potential to restore natural limb function and sensation [1-4]. Non-invasive PN interfaces wrap around the circumference of nerves reducing the risk of nerve damage and prolonging chronic performance [1-3]. Given their exterior location relative to the epineurium, these electrodes are largely insulated from the neural activity of individual axons, resulting in lower signal-to-noise ratio (SNR) and selectivity. Better access to the central axon population and improved targeting of smaller axon groups has been achieved using penetrating interfaces, but at the cost of greater invasiveness [5, 6].

LACE aims to achieve high fascicle selectivity while maintaining a minimally invasive interface by inducing collateral axonal sprouting from axons within the PN fascicles towards the microfluidic channels by way of targeted drug delivery. Lysing agents will be delivered to the fascicles closest to the microfluidic outlet ports to temporarily disrupt the epineurium, followed by delivery of neurotrophic factors to promote axonal sprouting towards electrodes embedded in the microfluidic channels [7-10]. The cuff incorporates an adjustable locking mechanism to ensure close-fitting of the interface to nerves of varying diameters and permit highly localized drug delivery. This method will help realize a chronically stable PN interface capable of high SNR recordings.

DESIGN

The polymer device supports pairs of Pt electrodes (geometric surface area of 0.45 mm^2) embedded within four Parylene C microfluidic channels (Design 1, 250 µm W × 20 µm H). The cuff is designed to fit securely around a rat sciatic nerve, and is held in position by etched serrations which accommodate diameters between 1.1 to 1.5 mm in 0.1 mm increments (Figure 1).

Two separate fluidic channel designs were investigated to improve mechanical robustness, particularly during deformation, and allow uniform flow through all channels in the curled orientation. Design 2 incorporates polymer support walls along the horizontal channel as shown in Figure 1b [11, 12]. Mid-channel support walls were fabricated from Parylene along the horizontal feeder channels at sites where channel collapse was previously observed. Design 3 incorporates microfluidic channels with narrower widths and lower aspect ratio (Figure 1c).

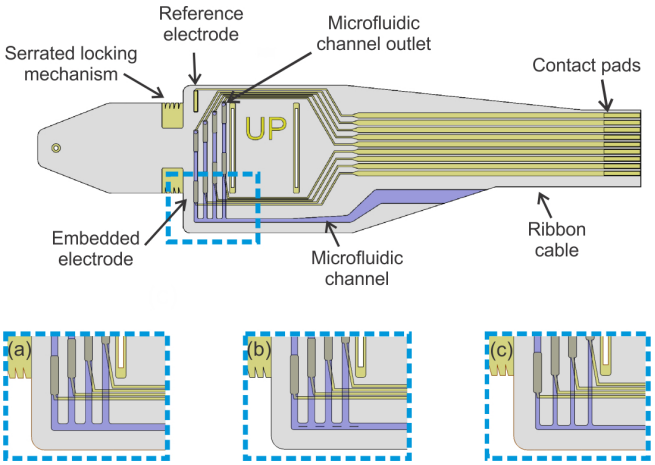

Figure 1: Schematic of LACE showing three different microfluidic channel configurations that support channel integrity when the cuff is curled: (a) Design 1: standard channels (20 µm H x 250 µm W), (b) design 2: incorporation of mid-channel supporting walls (20 µm H × 20 µm W × 390 µm L), and (c) design 3: narrower channels (150 µm and 250 µm W sections).

FABRICATION

Devices were batch fabricated using standard Parylene micromachining processes (Figure 2). Platinum was sputter deposited (2000 Å thick) and patterned on a Parylene coated (10 µm thick) silicon wafer by a lift-off process. Following deposition of a 10 µm Parylene insulation layer, sacrificial photoresist (20 µm height) was patterned to establish the microfluidic channel and the mid-channel support wall

structures. A final 8 µm thick layer of Parylene was used to enclose the microfluidics, and access ports were patterned and then opened with oxygen plasma.

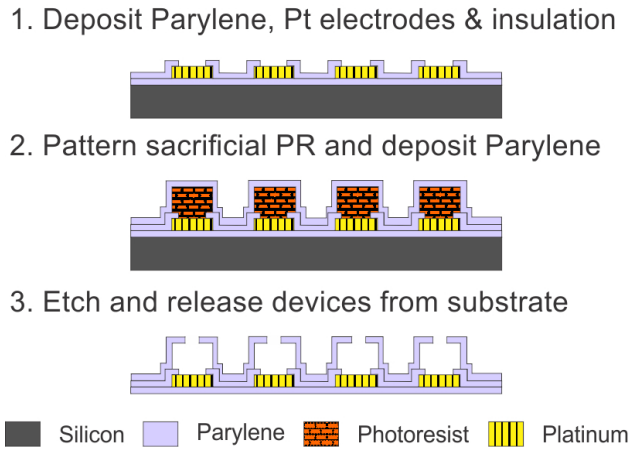

Figure 2: LACE fabrication process which utilizes standard surface micromachining techniques for Parylene.

Devices were released from the substrate and sacrificial photoresist was removed with an acetone soak (Figure 3). An electrical connection was established with a zero insertion force (ZIF) connector, using previously reported methods [13]. Device level fluidic packaging consisted of a polyether ether ketone (PEEK, part no. 1571, IDEX Health & Science) tubing secured in place with MED 4210 silicone adhesive (Factor II Incorporated).

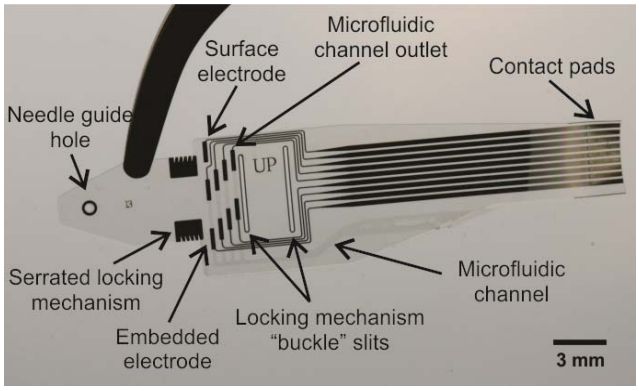

Figure 3: Photograph of fabricated LACE.

EXPERIMENTAL METHODS

Interlocking Mechanism Evaluation

A LACE device was wrapped around the sciatic nerve of an anesthetized 260 g rat and its holding strength was evaluated *in vivo* under handling conditions (Figure 4). The sciatic nerve was then dissected with the LACE device wrapped around it. All procedures for the animal experiments were in accordance with the animal protocol approved by the Animal Care and Use Review Office (ACURO).

Microfluidic Channel Evaluation

Microfluidic channels were evaluated in curled devices by infusing colored dye at a 500 nL/min flow rate using an external syringe pump (Harvard Apparatus Infuse/Withdraw PHD 2000) and imaging the transverse progression of the dye with a microscope (Caltex Scientific HD60T). Flat LACE devices were submerged in distilled water under the microscope, and primed by flushing the channels with isopropyl alcohol and distilled water for 5 minutes each. Devices were then curled, placed upright in an acrylic jig, and submerged under distilled water while infusing the microfluidic channels with a blue color dye.

Localization of fluid delivery was demonstrated by locking prototype LACE devices around a simulated sciatic nerve produced from a molded polydimethylsiloxane (PDMS) core covered with Kim-wipe, then driving blue color dye through the microfluidic channels using a syringe pump. The nerve phantom was selected to mimic the size of a rat sciatic nerve for the purpose of facilitating visualization during infusion studies. First, a PDMS core was cut from a block using an 18G coring needle (0.97 mm ID). This core was then circumferentially wrapped with two layers of Kim-wipe, increasing the diameter of the nerve phantom to approximately 1.3 mm, which falls in the sciatic nerve diameter range of 1.2 – 1.4 mm reported for a 340 g male rat. Devices were primed as previously described and then curled around the nerve phantom. Color dye was infused at 100 nL/min until it reached the fluidic outlet ports. The nerve phantom was imaged using an optical microscope and digitally processed using ImageJ (NIH) software to correlate the color signal with localization. The degree of localization of the infused fluid was quantified by the location and dimensions of the dyed area.

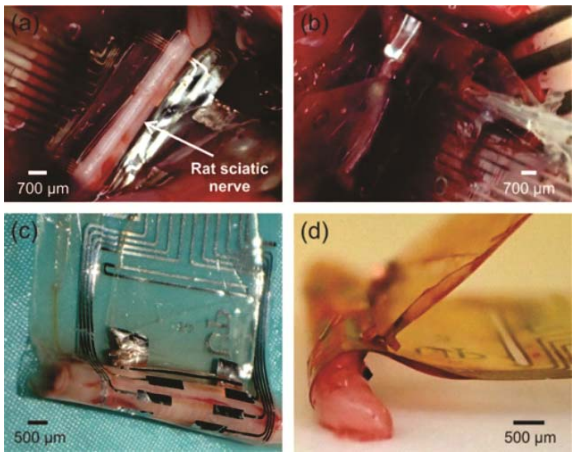

Figure 4: Photographs of the LACE placement on the sciatic nerve. (a) Unlocked LACE on the sciatic nerve, (b) locked LACE on the sciatic nerve, and (c-d) locked LACE on the dissected sciatic nerve.

Embedded Electrodes Evaluation

Electrochemical impedance spectroscopy (EIS) was used to assess the recording capabilities of the electrodes.

Electrochemical characterization of the electrodes was performed with a Gamry Reference 600 potentiostat (Gamry Instruments, Warminster, PA). The electrode surface was electrochemically cleaned with cyclic voltammetry (CV) in 0.05 M H_2SO_4 prior to EIS measurement. LACE devices were soaked in phosphate buffer saline (1× PBS) at room temperature under vacuum for 1 hours to prime the fluidic channels prior to EIS testing. EIS was performed with an AC perturbation signal of 10 mV (rms) in the frequency range of 1-10^5 Hz. An Ag/AgCl (3M NaCl) reference and 1 cm^2 Pt plate counter were used.

RESULTS AND DISCUSSION

Interlocking Mechanism Evaluation

The locking mechanism was simple to implement and robust; no damage to the nerve or cuff was observed when engaging and releasing the lock or after curling.

Microfluidic Channel Evaluation

Uniform flow through all fluidic channels and outlet ports was achieved with design 2 (n = 3) (Figure 5b). Flow through some channels was blocked by pinching of the horizontal feeder channel in designs 1 and 3 (Figure 5a & c). Design 2 will be selected for future animal testing.

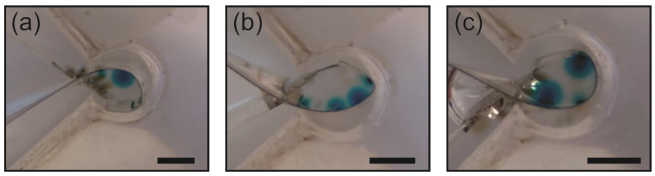

Figure 5: Representative photographs of the infusion experiment in curled devices at 500 nL/min flow rate (transverse view). The channels were primed with the dye introduced at the microfluidic inlet channel. (a) Design 1, (b) design 2, and (c) design 3. Scale bar is 1 mm.

Localized drug delivery on nerve phantoms was confirmed and is shown in Figure 6. Diffusion area was characterized by measuring the diameter of the outlet port stain using ImageJ software (Table 1). Localized delivery was achieved through at least three microfluidic channels with differing flow rates among individual channels. Consequently, the diffusion area for each channel is slightly different even within the same device.

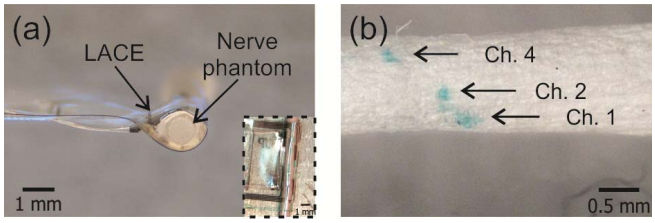

Figure 6: (a) Transverse view of LACE wrapped around a nerve phantom. Insert shows side-view. (b) Representative nerve phantom after localized dye delivery (n =3).

Table 1: Average diameter of outlet port stain (n = 3).

	Fluidic Port Diffusion Diameter (mean ± SE)
Device 1	0.209 ± 0.022 mm
Device 2	0.455 ± 0.058 mm
Device 3	0.310 ± 0.056 mm

Embedded Electrodes Evaluation

Electrochemical measurements on cuff electrodes yielded acceptable electrical impedance for the reference electrode for PN recordings. As expected, electrodes that were embedded in the channels exhibited higher impedance values which is attributed to the limited ion diffusion imposed by the surrounding fluidic channels (Table 2 and Figure 7). As these electrodes are intended to be used on axons that have grown into the microchannels, the increased impedance is not expected to adversely affect recordings. Instead, the close proximity of a specific axon is expected to improve nerve selectivity and signal fidelity.

Table 2: Electrochemical impedance spectroscopy in 1xPBS at 1 kHz (mean ± SE). Partially embedded electrodes are located underneath the fluidic outlet port.

Electrode	n	Impedance (kΩ)	Phase (°)
No fluidics	2	2.94 ± 0.43	-59.76 ± 9.66
Partially embedded	8	14.27 ± 1.38	-35.16 ± 3.81
Fully embedded	8	44.94 ± 8.50	-18.10 ± 3.08

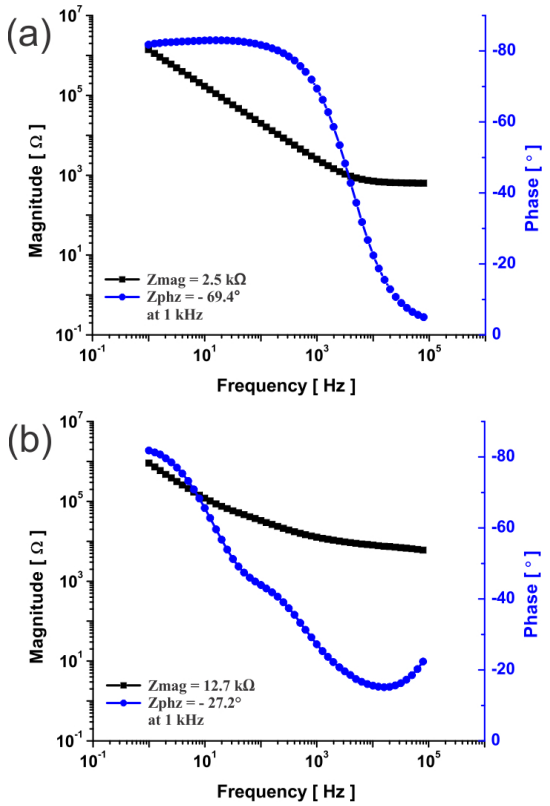

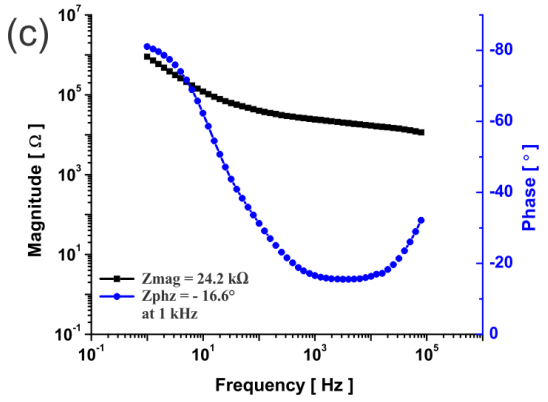

Figure 7: Representative electrochemical impedance spectroscopy plots of impedance magnitude and phase in 1xPBS for a (a) surface electrode with no fluidics, (b) partially embedded electrode (fluidic outlet port), and (c) fully embedded electrode.

CONCLUSION

We developed a novel Parylene-based PN interface with the potential to achieve improved SNR, recording selectivity, and prolong *in vivo* performance over existing technologies. The adjustable locking mechanism proved to be simple to implement and provided adequate holding strength when wrapping or unwrapping around the rat sciatic nerve. Redesigned microfluidic channels achieved uniform flow through all channels, which is important for targeting multiple fascicles within the nerve. Localized fluid delivered was achieved at low flow rates. High EIS impedance values obtained for the embedded electrodes are attributed to the limited ion diffusion of the channels. The close proximity of the axon to the electrode is expected to yield high quality neural recordings. Future work entails long-term characterization of electrodes in simulated *in vivo* conditions and *in vivo* animal testing.

ACKNOWLEDGEMENTS

This work was supported under DARPA cooperative agreement HR0011-15-2-0006, Viterbi School of Engineering Ph. D. Merit Fellowship (AC), and USC Provost Fellowships (CL). The authors would like to thank Dr. Donghai Zhu and the members of the USC Biomedical Microsystems Laboratory for their assistance with this project.

REFERENCES

[1] X. Navarro, T. B. Krueger, N. Lago, S. Micera, T. Stieglitz, and P. Dario, "A critical review of interfaces with the peripheral nervous system for the control of neuroprostheses and hybrid bionic systems," *Journal of the Peripheral Nervous System,* vol. 10, pp. 229-258, 2005.

[2] T. Stieglitz, M. Schuetter, and K. P. Koch, "Implantable biomedical microsystems for neural prostheses," *Engineering in Medicine and Biology Magazine, IEEE,* vol. 24, pp. 58-65, 2005.

[3] S. Micera, M. C. Carrozza, L. Beccai, F. Vecchi, and P. Dario, "Hybrid bionic systems for the replacement of hand function," *Proceedings of the IEEE,* vol. 94, pp. 1752-1762, 2006.

[4] P. M. Rossini, S. Micera, A. Benvenuto, J. Carpaneto, G. Cavallo, L. Citi, *et al.*, "Double nerve intraneural interface implant on a human amputee for robotic hand control," *Clinical neurophysiology,* vol. 121, pp. 777-783, 2010.

[5] T. Suzuki, N. Kotake, K. Mabuchi, and S. Takeuchi, "Flexible Regeneration-type Nerve Electrode with Integrated Microfluidic Channels," in *Microtechnologies in Medicine and Biology, 2006 International Conference on*, 2006, pp. 303-305.

[6] T. Stieglitz, H. Beutel, and J.-U. Meyer, "A flexible, light-weight multichannel sieve electrode with integrated cables for interfacing regenerating peripheral nerves," *Sensors and Actuators A: Physical,* vol. 60, pp. 240-243, 1997.

[7] B. Rydevik, M. D. Brown, T. Ehira, and C. Nordborg, "Effects of Collagenase on Nerve Tissue: An Experimental Study on Acute and Long-Term Effects in Rabbits," *Spine,* vol. 10, pp. 562-566, 1985.

[8] L. Isaacson, B. Saffran, and K. Crutcher, "Nerve growth factor-induced sprouting of mature, uninjured sympathetic axons," *Journal of Comparative Neurology,* vol. 326, pp. 327-336, 1992.

[9] W.-C. Liao, Y.-J. Wang, M.-C. Huang, and G.-F. Tseng, "Methylcobalamin facilitates collateral sprouting of donor axons and innervation of recipient muscle in end-to-side neurorrhaphy in rats," *PloS one,* vol. 8, p. e76302, 2013.

[10] P. Haninec, R. Kaiser, and P. Dubový, "A Comparison of collateral sprouting of sensory and motor axons after end-to-side neurorrhaphy with and without the perineurial window," *Plastic and reconstructive surgery,* vol. 130, pp. 609-614, 2012.

[11] C. H. Mastrangelo and G. Saloka, "A dry-release method based on polymer columns for microstructure fabrication," in *Micro Electro Mechanical Systems, 1993, MEMS'93, Proceedings An Investigation of Micro Structures, Sensors, Actuators, Machines and Systems. IEEE.*, 1993, pp. 77-81.

[12] T.-J. Yao, X. Yang, and Y.-C. Tai, "BrF 3 dry release technology for large freestanding parylene microstructures and electrostatic actuators," *Sensors and Actuators A: Physical,* vol. 97, pp. 771-775, 2002.

[13] A. Cobo, K. Scholten, J. Yoo, C. Larson, T. Hudson, V. Pikov, *et al.*, "A Parylene Peripheral Nerve Cuff Electrode with Integrated Microfluidics " presented at the 17th Conference on Solid-State Sensors, Actuators and Microsystems, Hilton Head, South Carolina, 2016.

CONTACT

*E. Meng, tel: +1-213-8213949; ellis.meng@usc.edu